SPT Dynamic Analysis and Measurements

By H. Abou-matar[1] and G. G. Goble,[2] Member, ASCE

Abstract: Measurements of force and acceleration on SPT systems are discussed and evaluated using solutions from both wave mechanics and a wave equation analysis program. The results show that acceleration and force can be accurately measured during SPT operations with currently available transducers, and that the force and particle velocity calculated by wave equation analysis agrees well with both measurements and wave mechanics solutions. A study of energy transmission in the SPT system is included. This study was conducted using wave mechanics and wave equation analysis. The results show that to accurately calculate energy transmission, measurements of both force and acceleration must be available. The method that has been specified in ASTM D4633-86 can produce large errors. The wave equation analysis also indicates that the standard penetration test (SPT) blow count is affeçted by drill rod area for low blow counts.

INTRODUCTION

The standard penetration test (SPT) is very widely used for subsurface investigation in many parts of the world. Because equipment and procedures are not very well standardized in the United States, considerable interest has been shown in evaluating the efficiency of the operation of the test (Schmertmann and Palacios 1979). Methods have been developed for measuring the energy transmitted to the rod and these methods have even been standardized (ASTM 1986).

In practice, problems are frequently encountered and questions are raised about the accuracy of dynamic measurements made at the top of the SPT rod. Studies of these measurements were made at the University of Colorado for several years (Hauge 1979; Chen 1990; Abou-matar 1990). In this paper, strain and acceleration measurements will be discussed and evaluated using one-dimensional wave mechanics and wave equation analysis. Measurement problems will be illustrated both analytically and experimentally and methods will be presented for detecting and avoiding these problems. Observations will be made regarding the use of measurements in the routine evaluation of SPT operations.

ANALYSIS OF STRESSES GENERATED IN SPT DRIVING SYSTEM

If reliable conclusions are to be reached on the efficacy of SPT operations using measurements performed on the drill rod, it is necessary to evaluate the correctness of those measurements. A procedure that can be used for the analysis of stress wave propagation in the SPT system using one dimensional wave mechanics will be presented. To gain confidence in the accuracy of drill rod measurements, this analysis can be applied to cases where measurements are made. It can also be used to examine errors in energy calculations.

When wave propagation is in one direction only in a uniform, homogeneous cross section rod, stress and particle velocity are proportional according to the relationship

$$\sigma = \frac{E}{c} v \tag{1}$$

where E = modulus of elasticity of the rod material; $c = \sqrt{E/\rho}$ = wave propagation speed (ρ = mass density of the rod material); and v = particle velocity in the rod at the same location as the stress, σ. At the beginning of SPT impact, the stress wave is usually assumed to travel in one direction only since there will be no reflections due to shaft resistance forces in the open bore hole. Thus, the first part of the measurement can be used to evaluate measurement quality. If force and particle velocity are proportional, then confidence is gained in the accuracy of the measurements. There may be upward traveling wave reflections from the drill rod connectors but these reflections usually will arrive after the first peak in the force and velocity measurement. If only a single measurement is made, for example force, as is specified in the ASTM energy measurement standard, then there is no way to evaluate the accuracy of the measurements and gross errors can result. [A thorough discussion of wave mechanics applications in analyzing impact was given by Fischer (1984).]

Experience gained from pile driving measurements shows that the maximum stress at impact is rarely greater than E/c times the impact velocity of the ram; this condition would be expected if the ram were effectively rigid compared with the pile. In laboratory tests on several SPT systems, stresses were often measured that were larger than the rigid ram result (Abou-matar 1990), a condition that is at first surprising but can be explained by wave mechanics evaluation of the impact stresses for real SPT driving systems.

When the SPT hammer impacts the drill rod, it creates a compression stress wave that travels down the rod and at the same time propagates in the hammer. Fairhurst (1961) describes what ideally happens when two rods impact. Across the plane of contact two conditions must be fulfilled during impact: (1) the contact forces in the hammer and the rod must be equal; and (2) the absolute spatial velocities of the striking end of the hammer and the struck end of the rod must be equal at all times when the two surfaces are in contact. From these conditions, the particle velocity in the rod and the hammer can be written in terms of the impact velocity v

$$v_h = \left(\frac{\alpha_h}{1 + \alpha_h}\right) v \tag{2}$$

$$v_r = \left(\frac{1}{1 + \alpha_h}\right) v \tag{3}$$

where v_h = particle velocity in the hammer; v_r = particle velocity in the rod; α_h = impedance ratio Z_r/Z_h, where $Z = EA/c$ is the impedance and the subscripts r and h refer to the rod and hammer, respectively.

A sudden change in the rod properties will impose a disturbance on the wave transmission. For example, if an increase or decrease in area is encountered by the oncoming wave, part of this wave will be transmitted and part will be reflected at the point of cross section change. To analyze the effect of a cross section change, equilibrium and continuity conditions are

[1]Goble Rausche Likins and Associates Inc., 4535 Rennaisance Parkway, Cleveland, OH 44128.

[2]Prin., Goble Rausche Likins and Assoc., Inc., 5398 Manhattan Circle, Boulder, CO 80303.

Note. Discussion open until March 1, 1998. To extend the closing date one month, a written request must be filed with the ASCE Manager of Journals. The manuscript for this paper was submitted for review and possible publication on March 11, 1994. This paper is part of the ***Journal of Geotechnical and Geoenvironmental Engineering***, Vol. 123, No. 10, October, 1997. ©ASCE, ISSN 1090-0241/97/0010-0921–0928/$4.00 + $.50 per page. Paper No. 8026.

imposed at the juncture; namely, the force and velocity on both sides of the juncture must be equal at all times. From these conditions force and particle velocity of the reflected and the transmitted waves can be calculated as

$$F_t = \frac{2\alpha}{1+\alpha} F_i; \quad v_t = \frac{2}{1+\alpha} v_i \tag{4a,b}$$

$$F_r = \frac{\alpha - 1}{1+\alpha} F_i; \quad v_r = \frac{1-\alpha}{1+\alpha} v_i \tag{5a,b}$$

where F and v = force and velocity, respectively; and the subscripts t, r, and i = transmitted, reflected, and incident waves, respectively. The quantity α = impedance ratio Z_2/Z_1, where indices 1 and 2 are for the incoming and transmitting sections, respectively.

These relations show that the transmitted wave always has the same sign as the incident one. The sign of the force and the velocity in the reflected wave is dependent on the impedance ratio α. If the cross section change is below the point where measurements are made, the reflected force and velocity will return to the point of measurement and disturb the stress-velocity proportionality of (1).

SAFETY HAMMER

Consider now an SPT hammer blow generated by a safety hammer driving a drill string of AW rods. In this study, the individual rods were 1.5 m long. A schematic of the test system is shown in Fig. 1. In (a), the hammer is lifted to a height of 0.76 meters and then dropped onto the top of the driving rod (b), in this case a solid rod of the same diameter as the outside diameter of the AW rod. Impact between hammer and rod occurs at point A. A compression stress wave is generated in the rod propagating downward with the speed c. Two stress waves are generated in the hammer emerging from the point of impact. One goes upward and is a compression wave; the other travels downward creating tension in the hammer shaft. The distance from the point of impact A to the top of the hammer B is very short, and since a free end reflection takes place at B the stresses in section A-B will cancel, due to superposition of waves, over most of the time of interest. For convenience and practical purposes, the part A-B can be ignored and only the tension wave traveling down the hammer is considered.

Four stages of wave propagation, shown in Fig. 2, will be

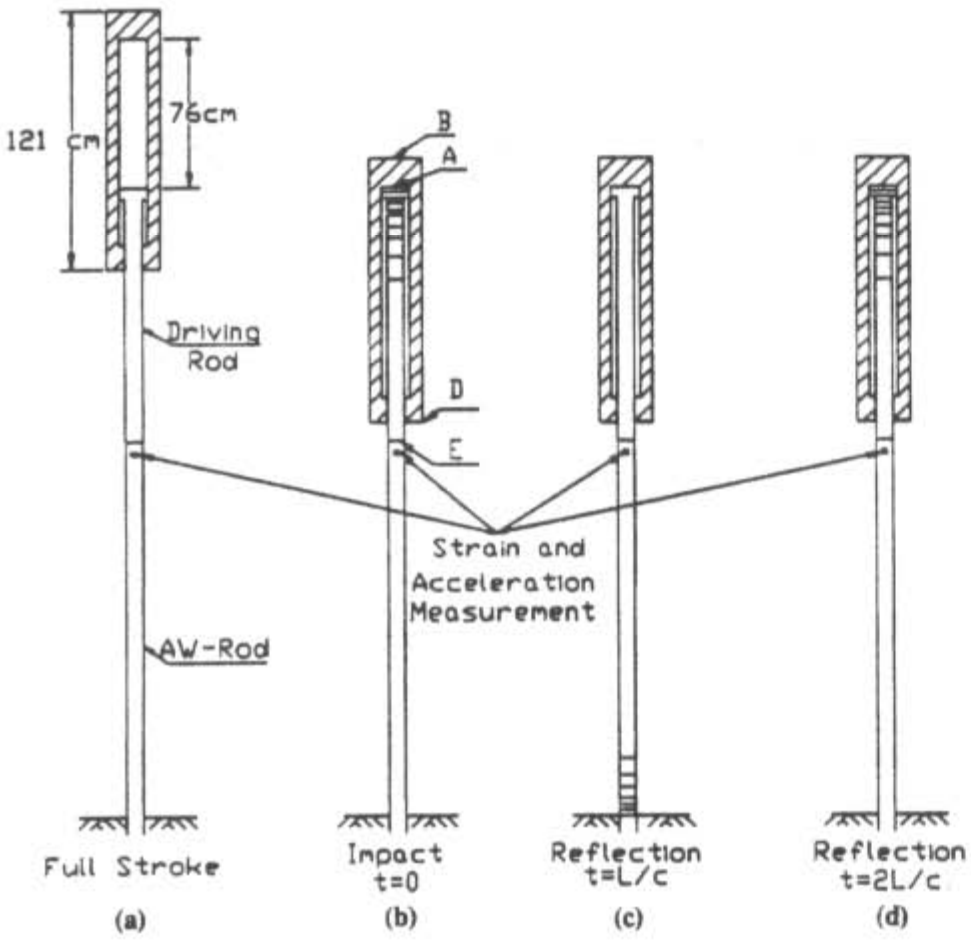

FIG. 1. Schematic of Blow in SPT with Safety Hammer

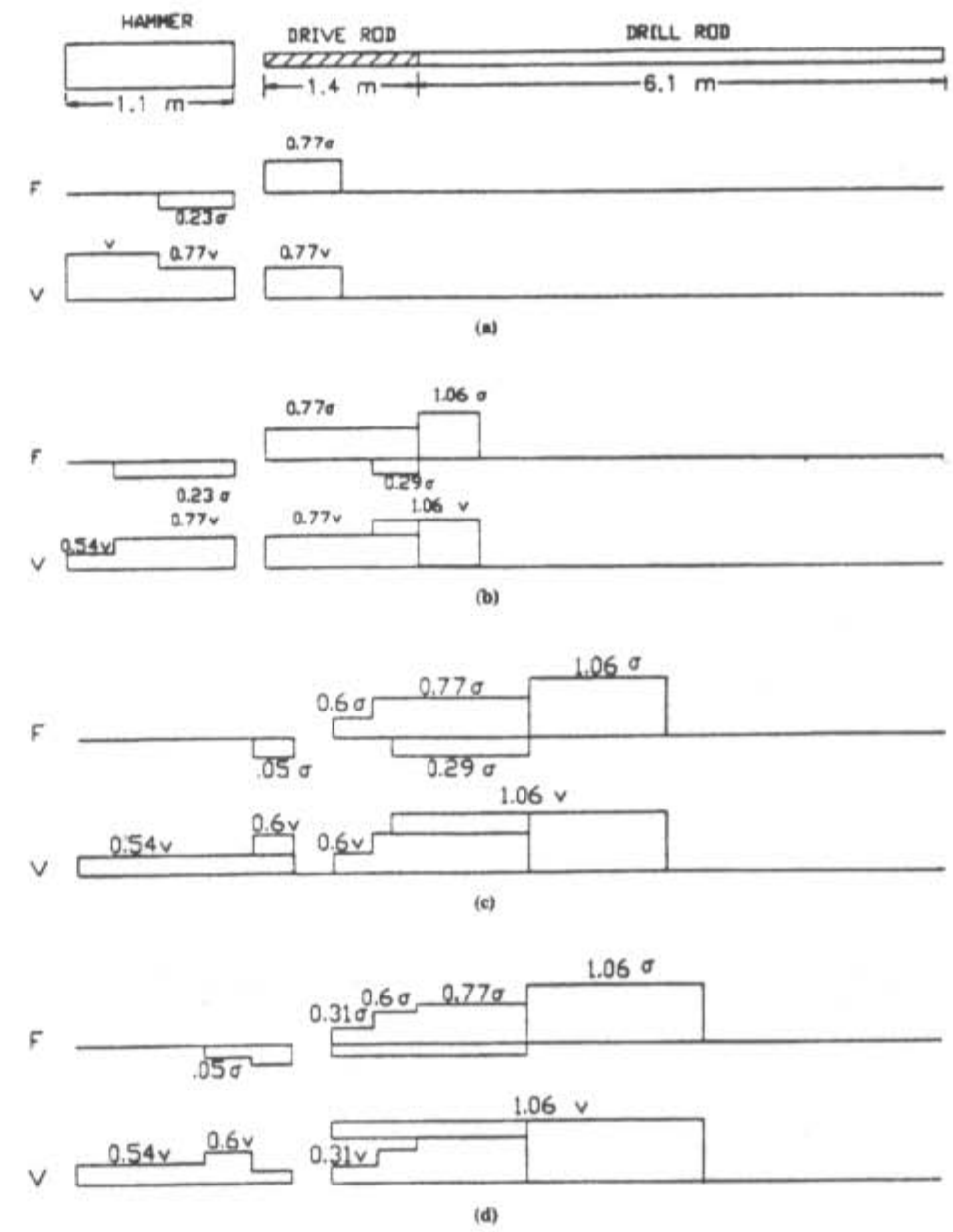

FIG. 2. Wave Propagation in Safety Hammer: (a) Just after Impact; (b) after Reflection from Hammer End and Drill Rod; (c) after Reflection from Hammer Impact Surface; (d) after Arrival at Impact Surface of Reflection from Drill Rod

discussed. The short line on the left side represents the ram of the safety hammer. The line on the right represents the drive rod, or anvil, which is solid and connected to an AW drill rod. Velocity and stress states in the system are plotted for several different times. The magnitudes of the velocity are given as a function of the impact velocity v of the ram. The stress is given as a function of σ, the ram impact velocity times the impedance of the cross section in question.

Since the hammer and the drive rod are fabricated from the same material, the impedance ratio α_h is the ratio of their cross-sectional areas, which in this case is 0.3. The particle velocity wave in the drive rod, generated as a result of the impact, can be calculated from (3) and has a magnitude $0.77v$. Just before impact, the particle velocity at all points in the hammer is equal to the impact velocity. At impact, this velocity will decrease by $0.23v$ [(2)] so that the particle velocity in the hammer equals that in the rod [Fig. 2(a)]. The same values will represent the stresses since at this stage of the process proportionality holds.

When the downward moving tension wave reaches the bottom of the hammer (Point D in Fig. 1 and the left end in Fig. 2) a free end reflection takes place. The additional mass at the bottom of the hammer is small compared to the hammer weight and the stress due to the inertia force of this mass is negligible. The tension wave reflects as a compression wave of the same magnitude canceling the oncoming tension wave [Fig. 2(b)].

At the juncture E between the drive rod and the AW rod, a decrease in area is encountered between two rods of the same material so the impedance ratio α equals the ratio between the areas, 0.46. This causes a reflection and transmission of waves according to (4) and (5), which indicate 63% of the arriving compression force transmitted as compression and 37% reflected as tension. From (4), the transmitted particle velocity is $1.37v_i$, where v_i in this case is the velocity in the drive rod,

which equals $0.77v$. Therefore, the transmitted velocity is $1.06v$ [Fig. 2(b)]. The transmitted wave propagates down the rod until it reaches the bottom where it is reflected according to the existing boundary conditions and travels back up the rod.

The reflection from the intersection between the drive rod and the drill rod is a tension stress of magnitude 0.29σ, which reduces the stress in the drive rod to 0.48σ. The reflected velocity is positive (downward) and adds to the velocity in the drive rod at which stage proportionality between stress and velocity no longer holds.

In the meantime, the free end reflection from the hammer bottom reduces the stress in the hammer to zero and further reduces the velocity by an additional $0.23v$–$0.54v$ [Fig. 2(b)]. When this velocity reaches the impact surface it reduces the input velocity to the drive rod producing a reduced force input [Fig. 2(c)]. At a slightly later time the tension reflection traveling up the drive rod is reflected as a tension wave, which will decrease the input stress in the drive rod [Fig. 2(d)]. The subsequent superposition of the many waves generated by the various section changes produces a very complex wave propagation pattern and will not be discussed further here.

Laboratory tests were performed at the University of Colorado on an SPT system with a safety hammer as described in Fig. 1. The hammer and anvil used were manufactured by the Central Mine Equipment Company (CME). A total of 6 m of AW rod was connected to the driving system and supported on the laboratory floor. The end of the bottom AW rod was welded to a flat plate that rested on sheets of plywood on the laboratory floor. The support conditions were quite soft since it was desirable to avoid damage to the floor and, in addition, there was no interest in examining more than the first $2L/c$ time period of the dynamic measurement. The AW rod consisted of 1.5-m sections connected together by one of the commercial connectors having a different area from that of the rod. The hammer was lifted the prescribed 0.76 m and then allowed to fall free by cutting the wire connection to the lifting hook.

The impact velocity was measured with a Hammer Performance Analyzer, a doppler radar-based device manufactured by Pile Dynamics, Inc. The strain was measured 150 mm below the top of the AW rod using foil resistance strain gauges attached directly to the AW drill rod. Acceleration was also measured at the same location as the strain with piezoresistive accelerometers manufactured by Entran, Inc. The strain and acceleration data was sampled digitally by a RC Electronics A/D recorder and stored in a personal computer. Acceleration was integrated to obtain velocity, which will be referred to as the measured velocity. The frequency response of this system was about 10 kHz as limited by the response of the bridge amplifiers that were used to condition both the strain and acceleration channels. This testing system has been described in greater detail by Abou-matar (1990).

The results of the measurements are shown in Fig. 3 plotted in force units (the velocity has been multiplied by the AW rod impedance, EA/c). Also shown in Fig. 3 is the force calculated by the theoretical procedure discussed earlier. Using the procedures developed for evaluating driven pile test data the correctness of the measurements can be examined. The measured force shows a somewhat sharper initial rise than the velocity, possibly because the velocity is obtained by integration of the acceleration. The measured force and velocity are seen to show quite good proportionality as evidenced by their agreement between points A and F. At point F, the reflection from the toe of the drill rod arrives at the measurement location.

The measured data and the theoretical analyses agree quite well. Of course, the measured rise time is more gradual since the theoretical vertical rise is physically impossible in a real mechanical system. In this case, the measured toe reflection arrival time and the theoretically predicted time of toe reflection arrival are very similar. All of these considerations support the conclusion that both the measurements and the theoretical evaluations are reasonable.

An additional comparison was made by calculating the force and the velocity using the discrete wave equation analysis computer program GRLWEAP (1991). The results for the calculated force and velocity values are presented along with the measured values in Figs. 4(a) and (b). The wave equation anal-

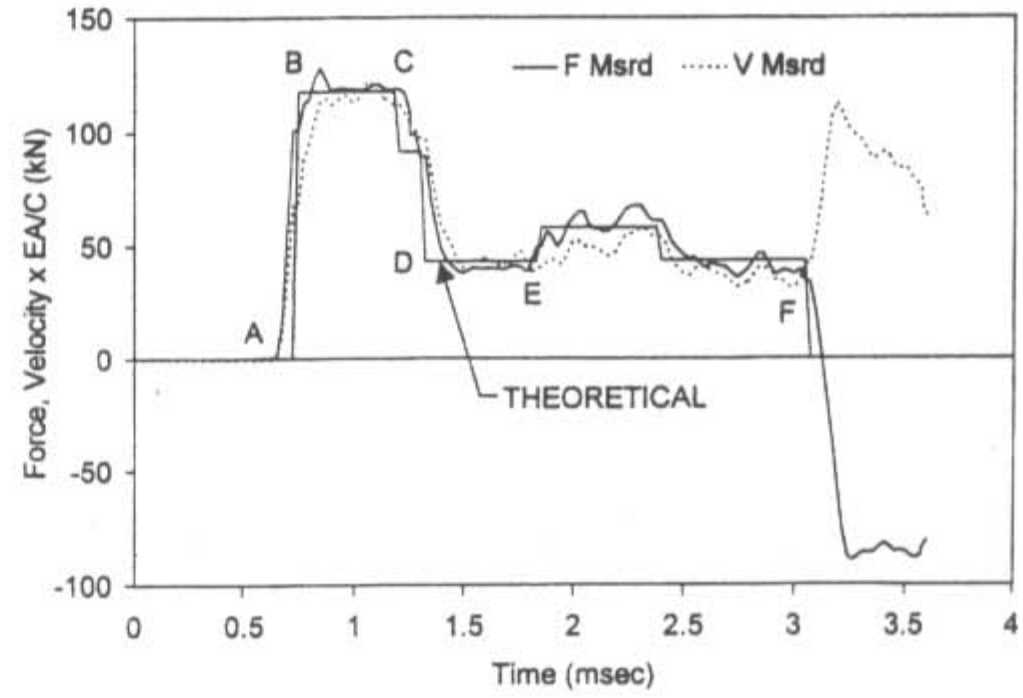

FIG. 3. Theoretical Wave Form Compared with Experimental Data

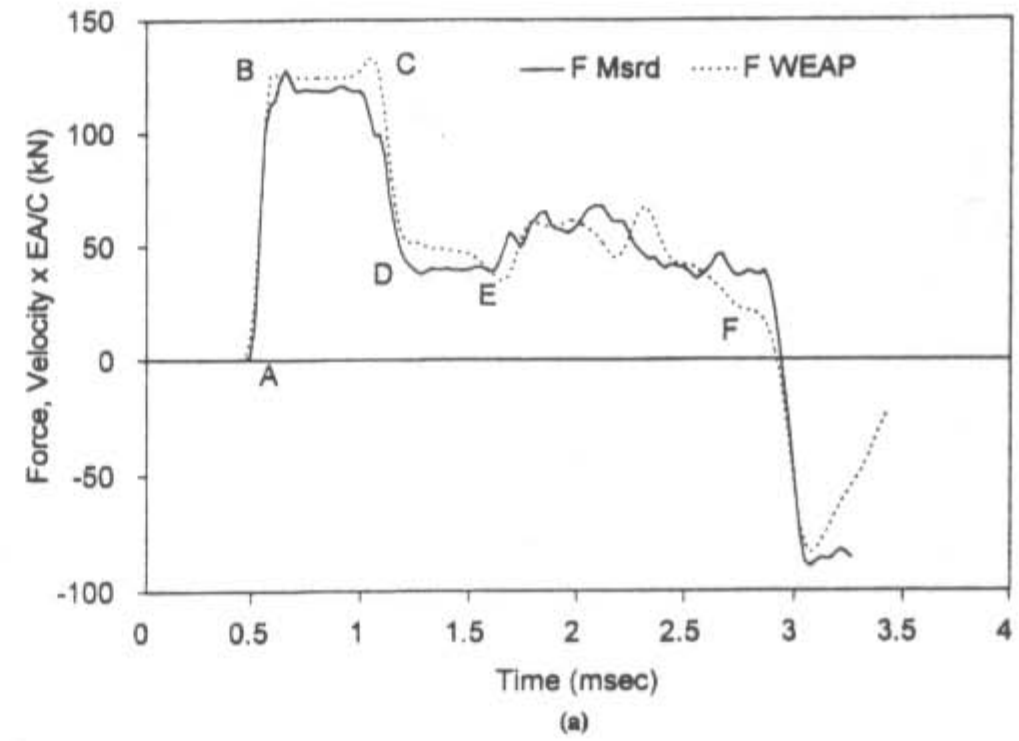

FIG. 4(a). Comparison between Force Calculated by GRL WEAP and Experimental Data

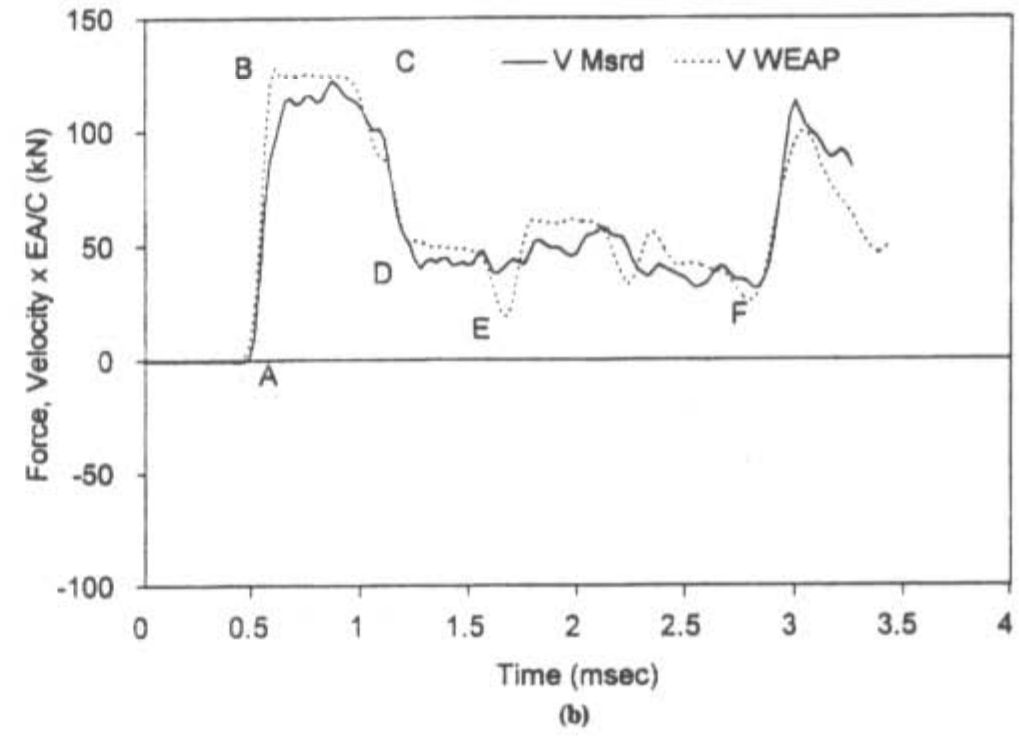

FIG. 4(b). Comparison between Velocity Calculated by GRL WEAP and Experimental Data

ysis was able to predict the force and velocity values in this steel-to-steel impact much better than had been expected. Very short element lengths (76 mm) were used in the analysis and the difference in the connector area was modeled in GRLWEAP, by representing the increased element mass and spring stiffness. In the actual test, the rod connections were carefully tightened to avoid slack. The maximum values at the first peak (point B) agreed very well. The departure from proportionality between the calculated force and velocity in the region of point C, in the GRLWEAP analysis, was due to the reflection from the first connector in the string of AW rods. The reflection from the second connector can be seen at point E in the GRLWEAP analysis. The absence of clear connector reflections in the measurements is probably due to the filtering of the measured signal.

When the WEAP program was originally developed it was extensively evaluated using measurements of strain and acceleration made during pile driving with a variety of hammers, piles, and driving systems. The results presented here indicate that a correctly modeled wave equation analysis can also be used to study SPT system performance.

CME AUTOMATIC HAMMER

As can be seen from this discussion, the magnitude of the stresses generated in the drill rod by a hammer blow is dependent on the geometry of the hammer and driving system. The CME automatic hammer is a mechanized single acting hammer, which consists of the standard 625 N ram that impacts on the top of an anvil connected to the drill rod. The dimensions of the ram and the anvil are shown in Fig. 5. The anvil is made of steel while the hammer is composite lead and steel. The impedance ratio α_h for their point of contact is 0.25.

Just before impact the ram is moving as a rigid body with a velocity equal to the impact velocity v. At impact, a part of this velocity is transferred to the anvil and a stress wave is generated, propagating downward in the anvil and upward in the ram. From (3), the velocity transferred to the anvil is $0.8v$ while that reflected to the ram is $0.2v$. The same values represent the stresses. The wave propagation in the system is shown in Fig. 6.

At the juncture of the anvil and the drill rod, transmission and reflection take place. The anvil and the drill rod are made of the same material and, thus, the impedance ratio is equal to their area ratio, which is 0.22. From (4) the transmitted

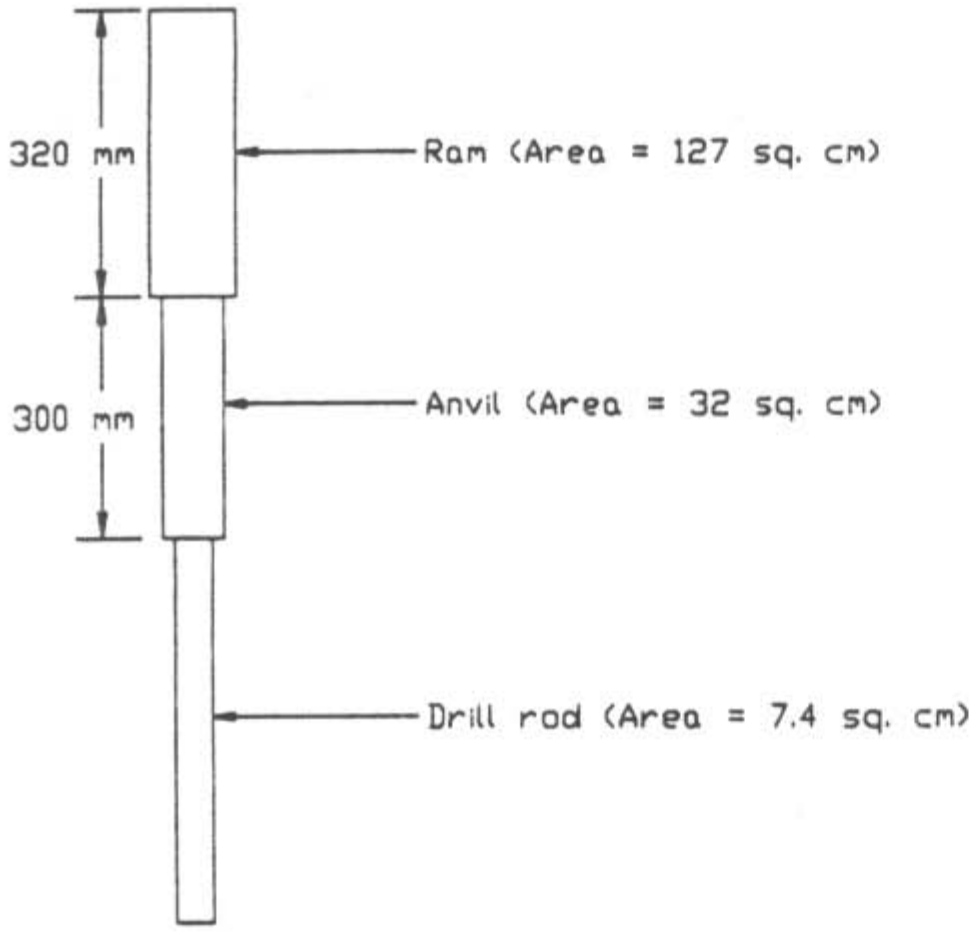

FIG. 5. Dimensions of CME Automatic Hammer

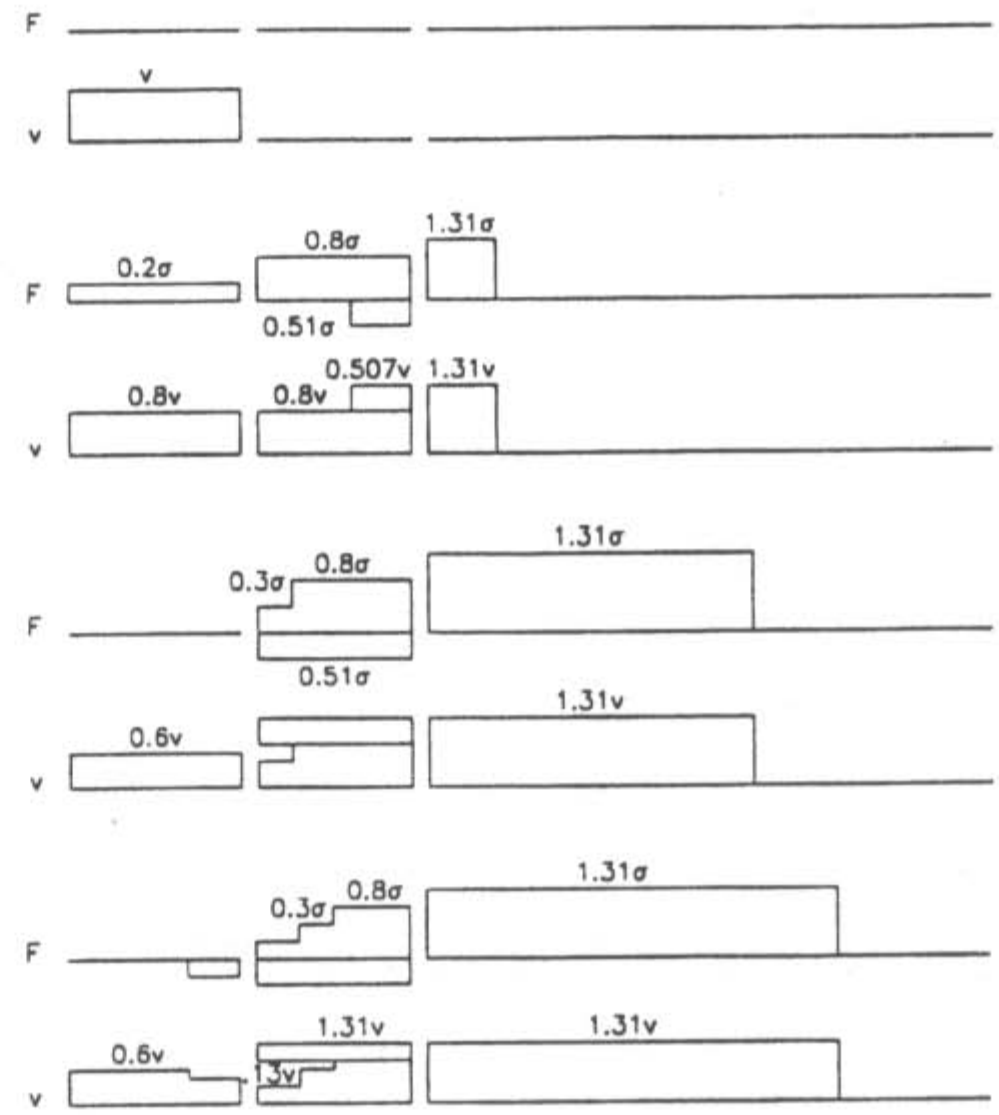

FIG. 6. Wave Propagation in CME Hammer System: (a) before Impact; (b) Just after L_{anvil}/c; (c) at $2L_h/c$; (d) at $2L_h/c + Dt$

velocity is $1.31v$ and the stress is 1.31σ. This value is 30% larger than that if the drill rod were struck directly by a rigid mass. Thus, the combination of ram, anvil, and rod areas behaves as an amplifier of the stresswave.

Measurements of force and velocity were made at a field site using a CME automatic hammer. The ram impact velocity was verified using the hammer performance analyzer. A sample of the force and velocity measurements is given in Figs. 7(a) and (b). A peak impact force of about 143 kN was measured. The impact velocity was measured as 3.88 m per second giving a theoretical force according to this analysis of 147 kN. The observed reflection from the toe at the $2L/c$ time is later than the theoretical one. This late arrival of about 0.3 ms is probably due to the existence of loose connections in the drill string. Extensive experience in pile driving measurements has shown that the wave speed in steel will not vary by measurable amounts. If there is a small slack in the rod, it must close before wave propagation can continue.

Force and velocity were calculated using the wave equation analysis program. The results are also shown in Fig. 7(a) and (b). They are seen to agree very well with the measured values except for some decaying cyclic variations after the first impact. It should be noted that the first peak after impact is generated by the dynamic interaction of the driving system elements.

If the anvil were removed and the ram dropped directly on the drill rod, the impact stress generated from such a blow would be smaller than with the anvil. The impedance ratio between the hammer and the drill rod is the ratio between their areas, 0.056. By substituting for this value in (2), the stresses in the rod for such a system would be $0.95\sigma_i$, where σ_i is the impact stress, which equals the impact velocity times the impedance of the drill rod. The high stresses generated by the system containing the anvil may not be desirable. In addition to the high compression stresses, large tension stresses are reflected from the bottom of the drill string in easy driving. One can assume that the maximum tension stress will be approximately equal to the compression stress peak minus the force that resists the sampler penetration. In soils with N-values less than 30, the sampler resistance force will usually be less than

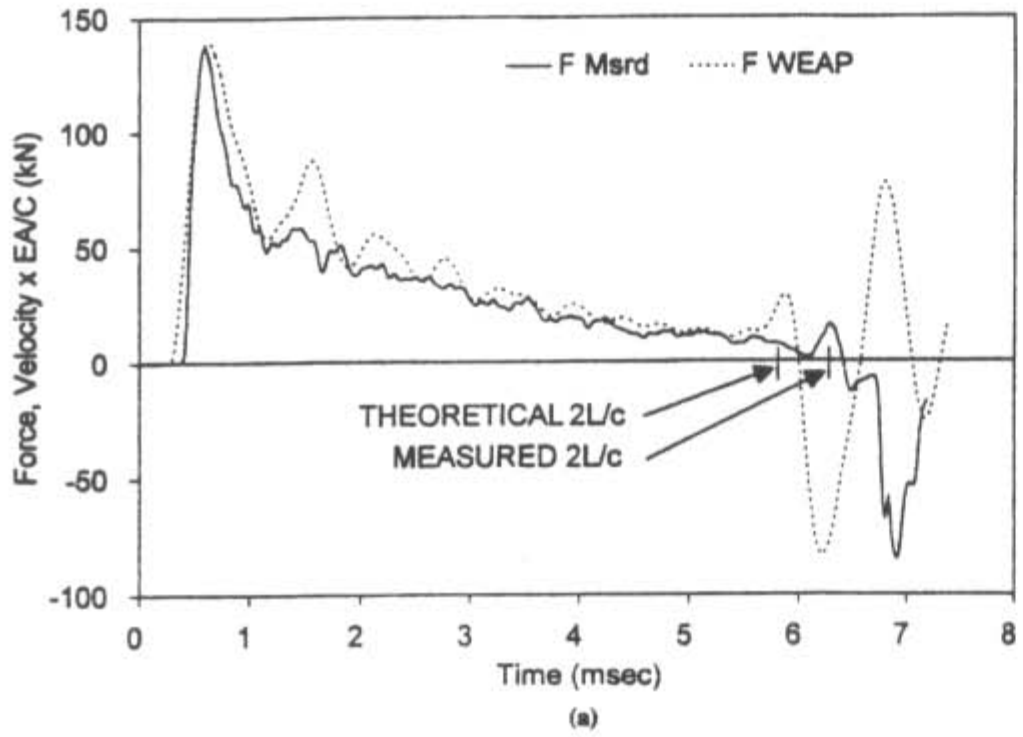

(a)

FIG. 7(a). Field Measurements and GRLWEAP Results Comparing Forces (Length below Gauges is 14.5 m)

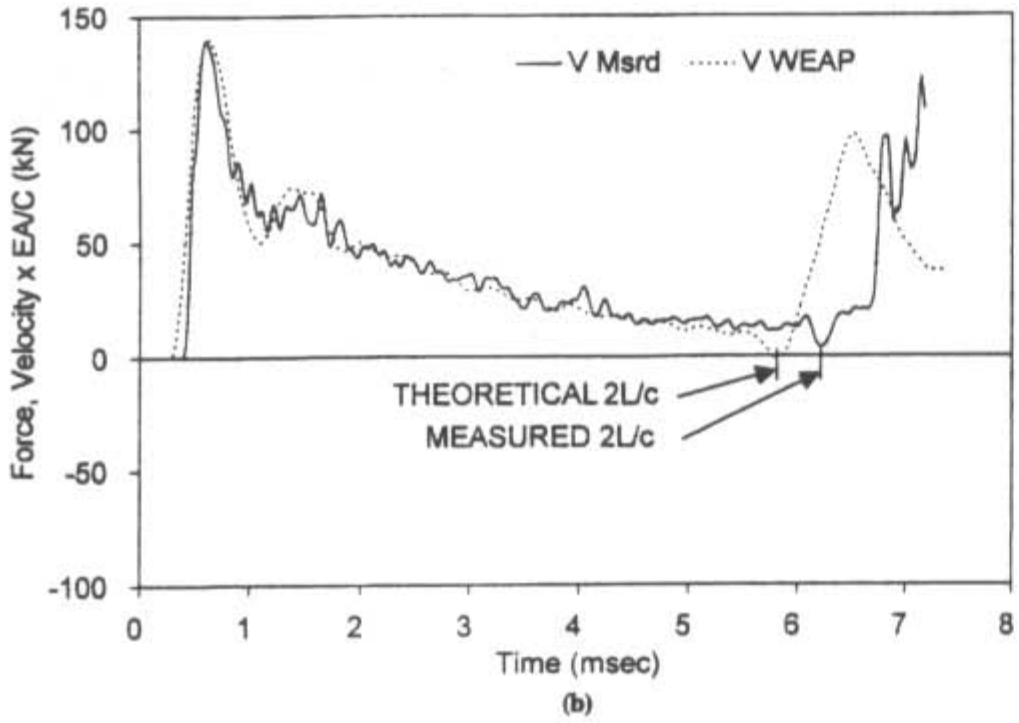

(b)

FIG. 7(b). Field Measurements and GRLWEAP Results Comparing Velocities (Length below Gauges is 14.5 m)

40 kN giving large stress cycles in each hammer blow. Thus, the drill string connectors will experience large stress reversals and this may cause the connectors to loosen. It may be desirable to reduce the area of the anvil, which of course would reduce the peak impact stress but not affect the total energy transmission.

Force and velocity, for the case where the ram impacted directly on the drill rod with no anvil present, were calculated using the wave equation analysis program. The rod length was 16.5 m with an additional length of sampler of 0.6 m. The results are presented later in this paper. The peak impact forces are about 37% lower than they would be if the anvil is used.

The examples of measured and calculated impact stresses discussed here give confidence in both the measurement equipment and the analytical method for stress calculation. Measured force and velocity were proportional, indicating that the currently used accelerometers give good results. In addition, the wave mechanics solution gave peak stresses and velocities that supported the measured values. The wave equation analyses agreed remarkably well with the measured results. It was impressive that it was possible to follow the very short rise times characteristic of steel-to-steel impact. These two analysis tools will be used later in this paper to examine some conditions that can realistically be encountered under field conditions.

PROBLEMS IN ENERGY MEASUREMENT AND CALCULATION

The measurement of energy transmitted to the drill string that was specified in ASTM Standard D4633-86 is of particular interest. This standard specified that the energy be calculated from the measured force by the relationship

$$e = \frac{c}{EA}\int_0^{t'} F^2(t)dt \tag{6}$$

where t' = time of the first zero value of the force signal. The calculated value for e was adjusted for errors arising from short rods and other factors, and the adjustment values were tabulated in the standard.

The basic relationship for calculating the energy contained in a stress wave up to some time t^* is

$$e(t^*) = \int_0^{t^*} F(t)v(t)dt \tag{7}$$

This relationship gives the energy as a function of time from the beginning of the wave when $t^* = 0$.

Eq. (6) is obtained from (7) by assuming that force and velocity are proportional according to (1). If this assumption is violated for any reason, the calculated energy will be incorrect. In what follows, energy transmission and some factors that cause force and velocity to lose their proportionality will be examined. The magnitude of the resulting error in the energy measurement will be determined.

DRILL ROD ENERGY TRANSMISSION

Questions are frequently raised regarding the transmission of energy in the drill rod—the energy transmitted to the soil and the displacement of the bottom of the rod are of particular interest. This can be examined and clarified using one-dimensional wave mechanics. Consider first a uniform cross section rod having a length L that is impacted in such a way that a rectangular compression wave of magnitude F_1 with propor-

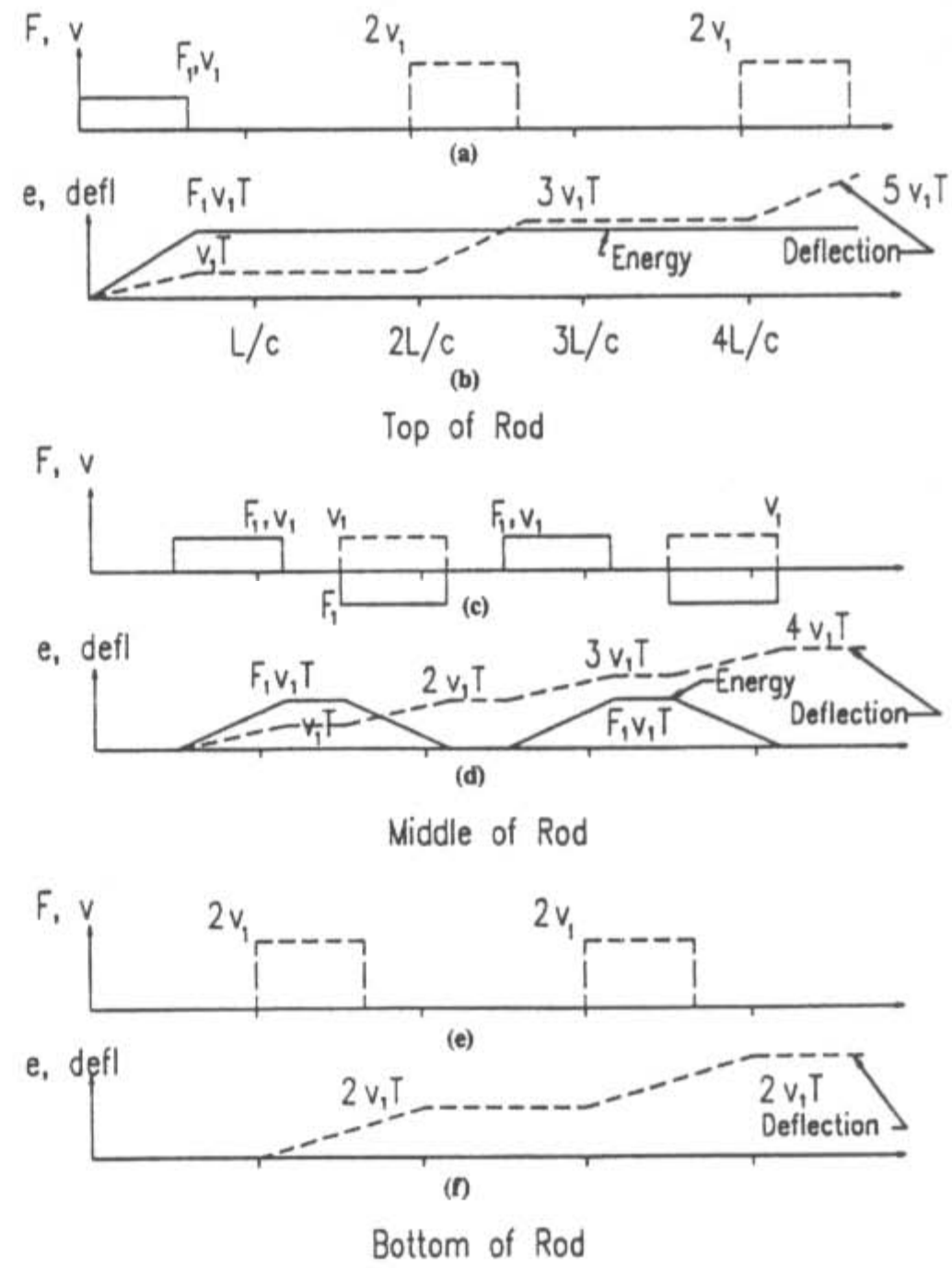

FIG. 8. Energy Transmission in Rod

tional velocity v_1 is generated at the top. The length of the stress wave is much less than the length of the rod and is such that it will travel past a point on the rod in time T. In this case, the bottom end of the rod is assumed to be free. The wave transmission observed at the impacted end of the rod is illustrated in Fig. 8 where (a) shows the force and velocity at the top of the rod and (b) gives the energy and displacement at the same location, both as functions of time. During the initial transmission of the wave, the energy and the displacement increase linearly and then remain constant until the reflection returns to the top. The top end is now free, the force must be zero, and the velocity doubles during wave reflection; since the force is zero no energy is transmitted out of the rod. During each reflection, however, the displacement increases as the rod moves ahead in pulses. The energy in the rod based on an observation at the top remains constant.

The same information is given for a point at the center of the rod. In Fig. 8(c), the force and velocity are shown. They are proportional during the first transmission and then the sign of the force changes at each subsequent reflection. The displacement [Fig. 8(d)] is seen to increase in ramps during each wave transmission since the velocity is always positive. The energy increases on the downward transmission and decreases again to zero on the upward transmission.

The conditions at the bottom of the rod are given in Figs. 8(e) and (f). Since the end is free there is no force and the velocity doubles during reflection. The rod end displaces in ramps like the top of the rod, but due to the zero force no energy is transmitted past the end of the rod. Thus, the energy remains in the rod and the wave reflects back and forth, only moving the energy around.

Now consider a case that is in all regards identical except that the rod has a resistance force of a magnitude 0.6 F_1 acting at the bottom of the rod when mobilized by rod motion (a condition like the SPT). This force is assumed to be rigid plastic as shown in Fig. 9(a) and to act only when the end of the rod is in motion. The wave transmission at the top is shown in Fig. 9(b) in the same manner as for the free end case. The first downward transmission is identical with the previous case. When the wave arrives at the end the resistance force is induced so the force at the end will be 0.6 F_1. The velocity is affected by the resistance force and can be determined from wave mechanics. The displacement and the energy transmitted past the top of the rod are given in Fig. 9(c). The wave transmission, the displacement and the energy transmitted past the center and bottom of the rod for the first $4L/c$, are also presented in Fig. 9. It can be seen that in the first wave transmission 84% of the energy in the rod is transmitted through the end of the rod by displacement of the bottom resistance force. On the second wave transmission, an additional 12% is transmitted.

It is interesting to note that energy transmission continues to the second cycle of wave propagation and then a small amount of energy is still in the rod. The magnitude of energy transmitted in the first wave arrival is dependent on the magnitude of the resistance force.

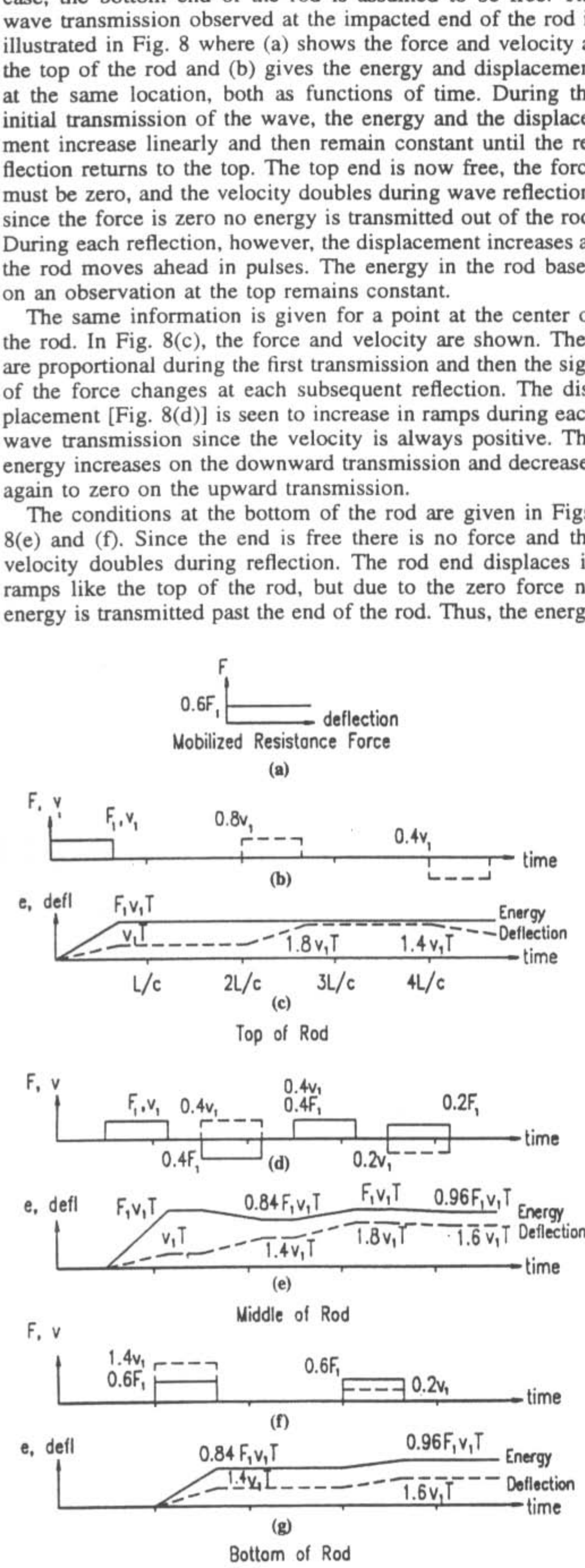

FIG. 9. Energy Transmission in Rod with Toe Resistance

PRACTICAL PROBLEMS IN ENERGY TRANSMISSION MEASUREMENT

Some practical problems in the measurement of energy in real SPT systems will be presented and discussed. In the aforementioned cases, the forces and velocities calculated by wave equation analysis have been shown to agree well with those determined by both wave mechanics and measurements. In what follows, wave equation analysis is used in a variety of cases to illustrate problems that can arise in the determination of the energy transferred to the drill string.

In the first case, consider the results presented in Fig. 10. A 16.5-m length of rod was impacted directly with the ram of the CME automatic hammer falling free from the standard drop height. The efficiency was taken as 100% with a coefficient of restitution of 0.9 and a total static resistance force of 13.4 kN was applied at the sampler together with the usual Smith damping constants for sand, 0.65 s/m for the shaft resistances, and 0.50 s/m for the toe with a quake of 0.8 mm. The soil constants are of little importance in the cases that will be presented since most of the emphasis is placed on that part of the record prior to the $2L/c$ time. The modeling of soil properties has been studied thoroughly by Goble and Aboumatar (1992) and Rausche et al. (1994).

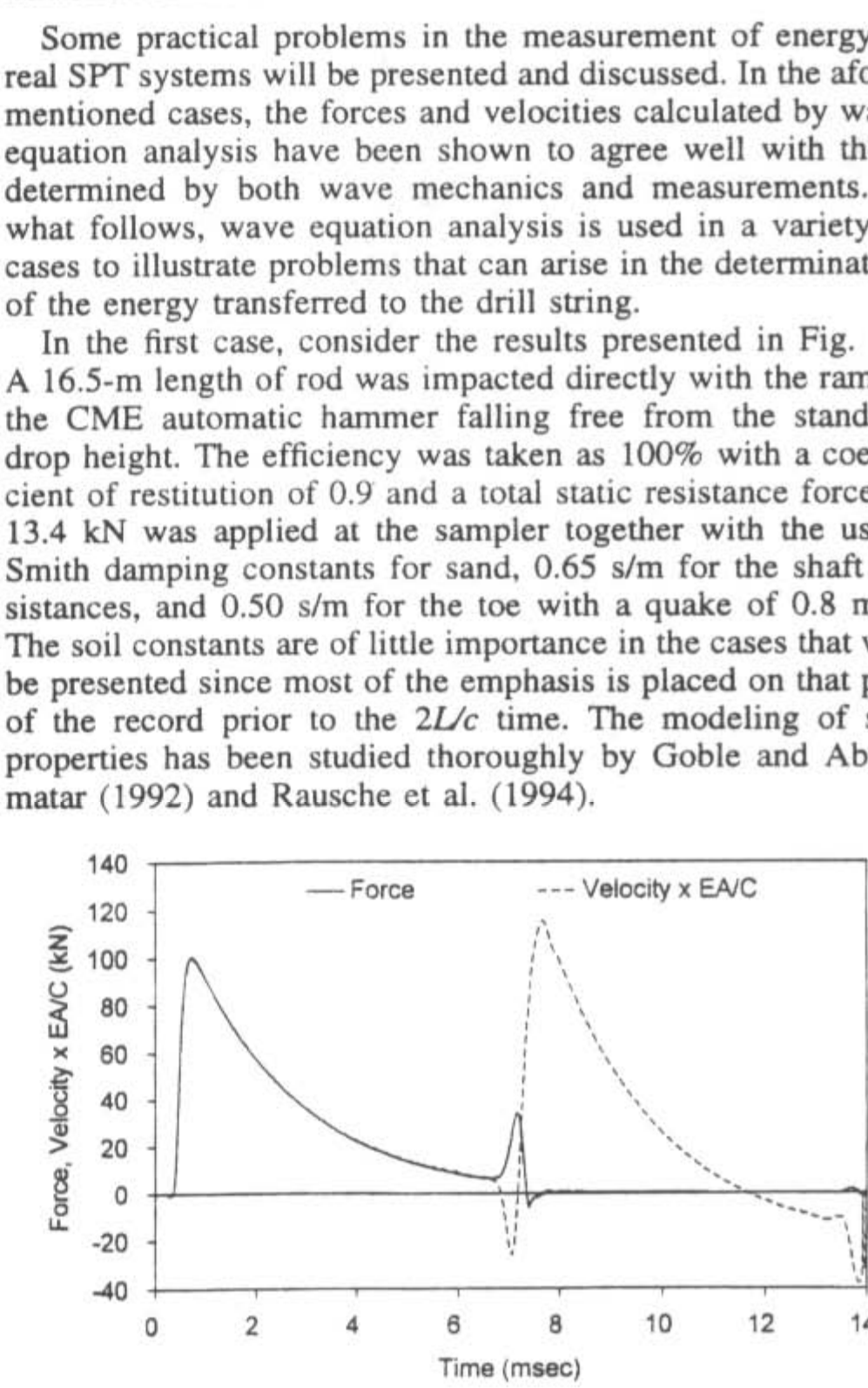

FIG. 10. Wave Equation Results for CME Hammer on AW Rod with no Connectors

The force and velocity curves in Fig. 10 were determined for a point 300 mm below the top of the rod. They were proportional until the reflection from the sampler returned to the top of the rod. Since the sampler had a larger area than the rod, the first reflection showed an increase in the force and a decrease in the velocity. Immediately following the sampler reflection the relatively small resistance force caused the top force to become zero and the velocity to increase to a large value. The force remained nearly zero since it was taken near the top, free end of the rod. The maximum value of the force at impact was 100 kN, indicating that the large cross-sectional area ram behaved as nearly rigid in this case. The force and velocity had decayed exponentially to near zero at the time of the sampler reflection.

The energy transferred to the drill rod according to both (6) and (7) was 472 J, slightly less than a perfect efficiency of 475 J. The force and velocity records indicate that some energy was still in the ram at the time of the arrival of the toe reflection. The blow count (N-value) according to the wave equation was 23 and 435 J, or 92% of the energy at the top was transmitted to the soil at the sampler.

The system described here was analyzed with connectors added to the drill rod, each having an area double the AW rod area and a length of 150 mm. The connectors were spaced at 1.5-m intervals. The results are shown in Fig. 11. The reflections from the connectors disturb the force-velocity proportionality causing the reflection of an increase in the force and a decrease in the velocity at each connector. The energy calculated from these records was 465 J from (7) and 508 J for (6). Thus, even the small connectors used here caused a difference of almost 10%, with the (6) result obviously in error and more than 100% efficient. The energy delivered to the soil was 394 J with a blow count of 25.

In Fig. 12, the case of the AW drill rod without connectors was analyzed with a CME anvil connected to the top of the drill string. This record should be compared with the result shown in Fig. 10. The only difference in this case is the presence of an anvil connected to the drill string so that the connection will carry tension. The peak impact force in the drill rod has increased due to the presence of the anvil, as was discussed earlier. Also, the force does not decrease monotonically, but shows two successive peaks following the initial peak at impact. Since the disturbance came from above, force and velocity remain proportional. The energy calculated near the top of the drill rod was 468 J for both (6) and (7) and the blow count was 24. The peak tension force reflected from the bottom of the drill string was much larger than for the case with no anvil. When a substantial mass exists above the point where the measurements are made the reflected tension force can be large. However, when the observation point is at or near a free end, a tension will not be observed.

This case illustrates the need of both force and velocity measurements. The force record was radically changed by the addition of an anvil attached to the top of the drill string. If velocity followed force as shown, the record would be proven correct. Without both force and velocity there is no way to verify measurement quality.

The performance of the Mayhew rod was examined and the results are given in Figs. 13 and 14. The Mayhew rod has an area more than twice the area of the AW rod. In addition, it has long, heavy connectors. First, the heavier rod without connectors or anvil was analyzed with all other input the same. Only the rod was changed. The force and velocity decayed more rapidly than for the AW rod and the peak values at impact were also larger due to the larger rod area. The energy delivered to the top was 473 J for both (6) and (7). However, only 354 J, or 75% of the energy was transmitted to the soil. The blow count was 35 blows per ft.

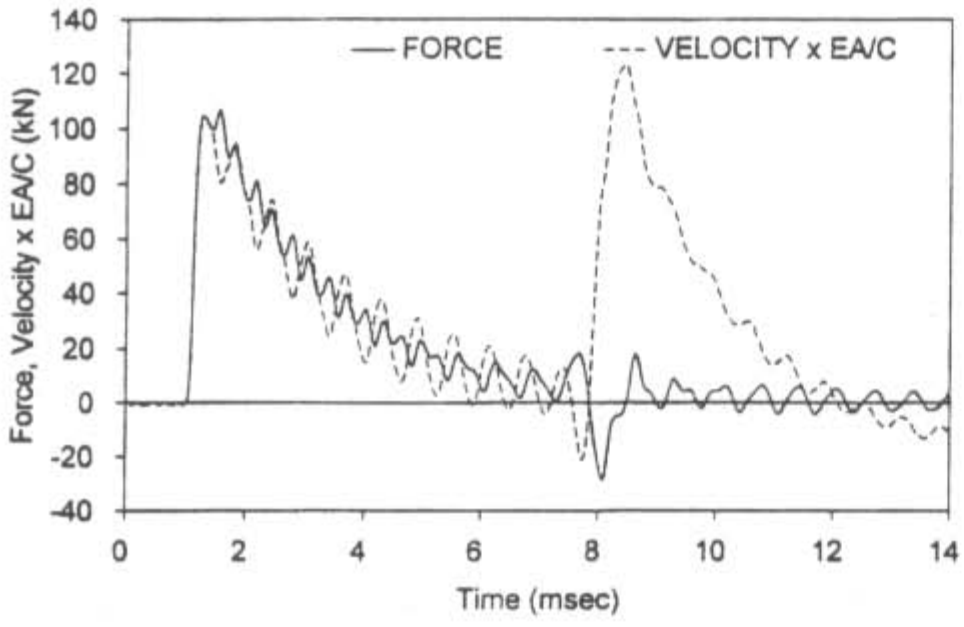

FIG. 11. Wave Equation Results for CME Automatic Hammer with Connectors at 1.5-m Intervals

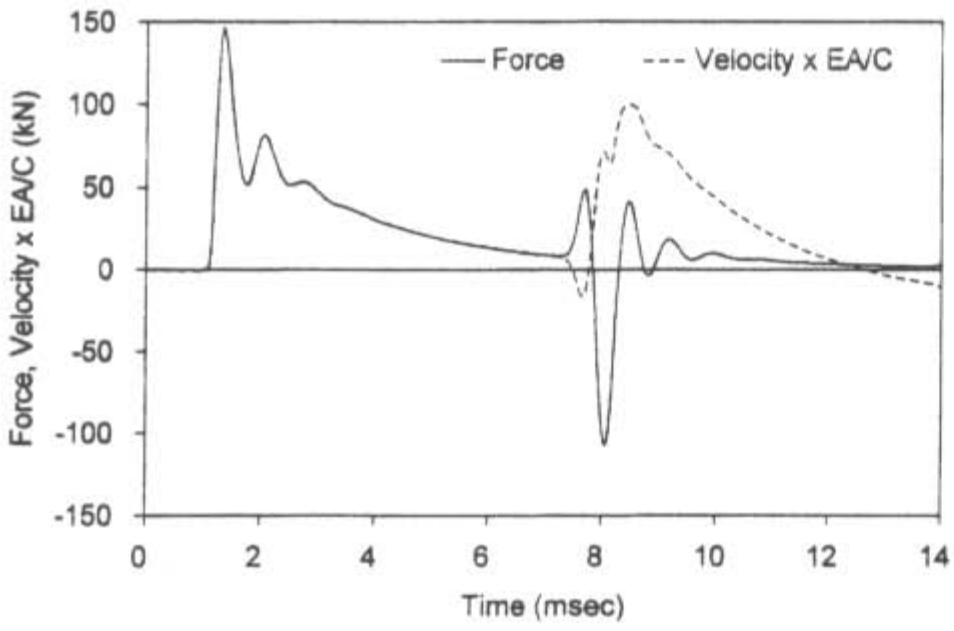

FIG. 12. Wave Equation Results for the CME Automatic Hammer on AW Rod with Anvil Attached

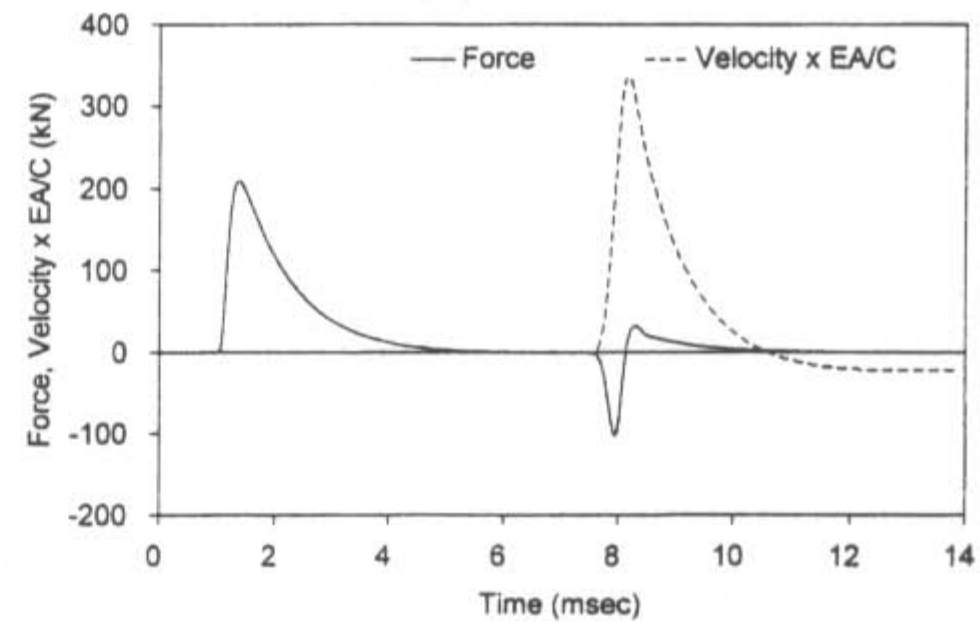

FIG. 13. Wave Equation Results for CME Hammer on Mayhew Rod No Connectors

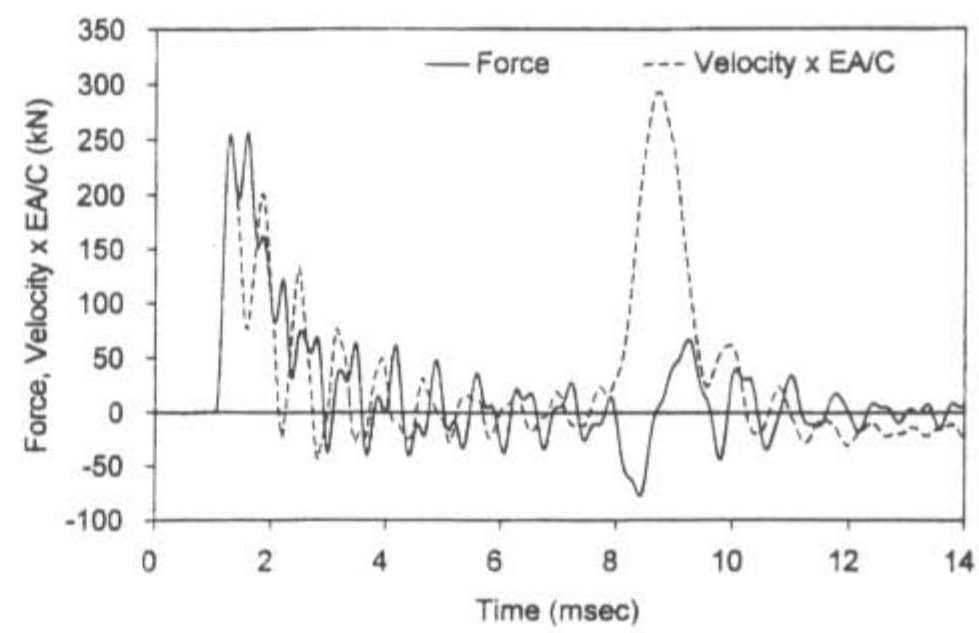

FIG. 14. Wave Equation Results for CME Hammer on Mayhew Rod, with Connectors

The analysis of the Mayhew rod with connectors is shown in Fig. 14. The large connectors cause large compression reflections and severe departures from proportionality after the first peak. The energy transmitted to the rod according to (7) was 462 J. Using (6) and stopping the calculation at the first zero in the force record as specified in ASTM D4633-86 gave an energy of 586 J or 20% greater than the theoretical maximum. The blow count was 41 blows per foot. A total of 313 J, or 66% of the energy, was transmitted to the soil. If the results of this case are compared with the case of the AW rod shown in Fig. 10, it can be seen that the force curve decays much more rapidly for the larger rod. This behavior would be expected since the decay rate is dependent on the impedance of the rod. In ASTM D4633-86, the correction for rod length was related to length only. It should also be dependent on rod cross-sectional area.

These examples illustrate the usefulness of wave equation analysis in examining SPT behavior. It is possible to vary a single quantity and clearly see the result in a way that would not be possible with a field test. It was shown that reflections from changes in rod cross-sectional area can cause serious errors in energy calculation if (6) is used. The increased blow count for the heavier rods was of particular interest. Supporting that result is the smaller energy delivered to the soil. This behavior can be explained by the results of the energy transfer illustration presented in Fig. 9. If the rod area is increased, then it can be expected that the forces in the rod will be larger for a given set of displacements, and therefore these forces would retain more energy in the rod. Of course, this result is quite disturbing. Definite conclusions, however, should await experimental confirmation of these results.

CONCLUSIONS

Laboratory measurements of force and acceleration on SPT systems have been examined analytically using solutions from both wave mechanics and wave equation computer analysis. Good agreement was obtained between the measurements and both analytical procedures. Also, the measurements proved to be correct since measured force and velocity showed good proportionality at impact. These observations support the following conclusions:

1. Acceleration can be measured accurately in the steel-to-steel impact conditions of SPT operations. Without both force and acceleration measurements it is not possible to evaluate the quality of the dynamic measurements.
2. Wave equation computer analysis can be used to accurately simulate the energy transmission in particular SPT systems.

Energy transmission in the SPT system was examined experimentally, by wave mechanics, and with wave equation analysis. The effect of drill rod cross section changes on the calculation of energy was examined using the three different approaches. It can be concluded that:

1. Small changes in cross section due to connectors in typical AW rods can produce errors of 10% in energy calculations using the approximate method of (6). For many other drill rod systems the error will be much greater.
2. The method of (7) gives good results for even the most extreme cases of rod cross-section variation. No corrections or limitations must be imposed.
3. To evaluate the validity of field measurements, the force and velocity records should be viewed as the data is taken to detect any measurement errors and take corrective action.
4. The method of (6) cannot be used for energy measurement in SPT systems unless limitations are put on the rod cross-section variations. The correction for rod length should also include rod area.
5. The analytical evaluation of energy transmission in a drill rod shows that the resistance to penetration of the rod will affect the magnitude of the energy transmitted into the soil.
6. The results of wave equation analysis indicate that the cross-sectional area and weight of the SPT drill rod may cause substantial change in the measured N-value. Controlled field testing should be used to verify this conclusion.

It is possible to accurately measure the energy transmitted to the drill rod using force and velocity measurements. These measurements should be subjected to the standard procedures used for evaluating pile driving measurements.

ACKNOWLEDGMENTS

The work presented here is the result of a continuous research project carried on at the University of Colorado for more than ten years. Financial support was obtained from the Central Mine Equipment Company, the Colorado Division of Highways, the Bureau of Reclamation, the National Institute of Standards and Technology, and GRL and Associates. The writers would particularly like to recognize the support, encouragement, and advice received from Charles Riggs, Sverdrup Corporation (formerly with the Central Mine Equipment Company); Charles Rassieur (deceased), Central Mine Equipment Company; Brandon Gilmore, Colorado Division of Highways; Jeff Farrar, Bureau of Reclamation; Felix Yokel, National Institute of Standards and Technology; Frank Rausche, GRL and Associates; and Garland Likins, Pile Dynamics. The Colorado Division of Highways was always cooperative in providing testing opportunities when their drill rigs were in the field, in spite of many cases of poor results and test failures. The reviewers offered extensive comments that substantially improved the coverage, clarity, and style of the paper.

APPENDIX. REFERENCES

Abou-matar, H. (1990). "Evaluation of dynamic measurements on the standard penetration test," Thesis presented to the Univ. of Colorado at Boulder in partial fulfillment of the degree of MS.

Chen, C. (1990). "Energy transfer in the standard penetration test," Thesis presented to the Univ. of Colorado at Boulder in partial fulfillment of the degree of MS.

Fairhurst, C. (1961). "Wave mechanics of percussive drilling." *Mine and Quarry Engrg.*, (March), 122–130.

Fairhurst, C. (1961). "Wave mechanics of percussive drilling." *Mine and Quarry Engrg.*, (April), 167–178.

Fairhurst, C. (1961). "Wave mechanics of percussive drilling." *Mine and Quarry Engrg.*, (July), 327–328.

Fischer, H. C. (1984). "Stress wave theory for pile driving applications." *Proc., Second Int. Conf. on the Application of Stress Wave Theory on Piles*, Commission on Pile Res., Royal Swedish Acad. of Engrg. Sci., Stockholm, Sweden, 1–78.

Goble, G., and Abou-matar, H. (1992). "Determination of wave equation soil constants from the standard penetration test." *Proc., Fourth Int. Conference on the Application of Stress-Wave Theory to Piles*, The Hague, The Netherlands, 99–103.

Goble Rausche Likins and Associates, Inc. (GRLWEAP). (1991). "GRLWEAP—wave equation analysis of pile driving." Cleveland, Ohio.

Hauge, K. (1979). "Evaluation of dynamic measurement system on the standard penetration test," Thesis presented to the Univ. of Colorado at Boulder in partial fulfillment of the degree of MS.

Rausche, F., Likins, G., and Goble, G. (1994). "A rational and usable wave equation soil model based on field test correlation." *Proc., Int. Conf. on Des. and Constr. of Deep Found.*, 1118–1132.

Schmertmann, J., and Alejandro Palacios. (1979). "Energy dynamics of SPT." *J. Geotech. Engrg. Div.*, ASCE, 105(8), 909–926.

Standard test method for stress wave energy measurement for dynamic penetrometer testing systems; D4633-86, ASTM, West Conshohocken, Pa., 775–778.